NanoTrapS
Trapped nanoparticles for space experiments
(AO/1-6889/11/NL/CBi)

	Name/Title	Signature	Date
Prepared by:	Rainer Kaltenbaek University of Vienna		31.03.2014
Study authors:	Philipp Schmid, Ugur Sezer, Johannes Horak, Markus Aspelmeyer, Markus Arndt, and Rainer Kaltenbaek		
Affiliation:	Vienna Center for Quantum Science and Technology, Faculty of Physics, University of Vienna		
Technical management:	Eric Wille TEC-MMO		
Vienna Center for Quantum Science and Technology Faculty of Physics, University of Vienna Boltzmanngasse 5, 1090 Vienna, Austria			

EUROPEAN SPACE AGENCY
FINAL REPORT
The work described in this report was done under ESA contract.
Responsibility for the contents resides in the author or
organisation that prepared it.

Page intentionally left blank

ESA STUDY FINAL REPORT		
ESA Contract No: AO/1-6889/11/NL/CBi	SUBJECT: Trapped nanoparticles for space experiments	CONTRACTOR: UNIV WIEN EXPERIMENTALPHYSIK BOLTZMANNGASSE 5 1090 WIEN
ESA CR()No:	No. of Volumes:.... This is Volume No:....	CONTRACTOR'S REFERENCE:

ABSTRACT

One of the challenges in physics today is to gain a better understanding of the laws of physics at the intersection of quantum and gravitational physics. As technology continues to push the apparent limits of the quantum world towards a macroscopic scale, matter-wave interferometers with increasingly massive objects may eventually allow for tests in this parameter regime. But, the higher the mass, the longer the typical free-fall time in matter-wave interferometry. Based on today's knowledge, reaching that border-line regime of quantum theory therefore also means reaching for the micro-gravity of a space environment. Atom interferometers, e.g., have by now already reached a TRL on the verge of being space proof. In order to achieve a comparably high TRL for matter-wave interferometry with more massive objects like macromolecules and nanoparticles, further technology development is necessary. While novel methods of detection and of high-mass matter-wave interferometers have shown impressive progress over the last decades, similar progress has yet to be achieved for high-mass particle sources. In the present study, we experimentally investigate several sources of macromolecules, clusters and nanoparticles that may be suited for future space-based matter-wave experiments. The source concepts investigated are laser desorption (LD), laser-induced acoustic desorption (LIAD), matrix-assisted laser desorption (MALD) and desorption via high-frequency surface-acoustic waves (SAWs). We present the designs of sources based on these mechanisms and the technical requirements they have to fulfill for future space-based experiments. In a series of experiments, we have investigated the working principles of these source mechanisms, the source characteristics for LD, LIAD and MALD, and we demonstrated trapping of particles produced by MALD. The investigated source mechanisms cover a mass range of $10^4 - 10^{11}$ atomic mass units. By increasing the TRL of source mechanisms for future matter-wave experiments over a wide mass range, our work is a significant step towards testing the foundations of physics over a wide and largely unexplored parameter range between the quantum and the classical world.

The work described in this report was done under ESA Contract. Responsibility for the contents resides in the author or organisation that prepared it.

Names of authors: Philipp Schmid, Ugur Sezer, Johannes Horak,
Markus Aspelmeyer, Markus Arndt, and Rainer Kaltenbaek

NAME OF ESA STUDY MANAGER: Eric Wille, TEC-MMO DIV: DIRECTORATE:	ESA BUDGET HEADING:

Page intentionally left blank

Table of Contents

1 List of Abbreviations **7**

2 Introduction and Motivation **9**

3 The proposed experiments **11**
3.1 DECIDE . . . 11
3.2 OTIMA . . . 13

4 Source designs and technical requirements **15**
4.1 Technical requirements for the particle sources . . . 16
4.2 OTIMA sources . . . 16
4.2.1 LD and LIAD . . . 16
4.2.2 MALDI TRAP . . . 18
4.3 SAW-based particle source . . . 20

5 Testing and characterization of the particle sources **23**
5.1 SAW-based particle source . . . 23
5.2 Laser desorption (LD) . . . 24
5.3 Laser induced acoustic desorption (LIAD) . . . 25
5.4 MALDI TRAP . . . 25

6 Trade-off, Conclusions & Discussion **27**
6.1 Trade-off . . . 27
6.2 Conclusions & Discussion . . . 28

Bibliography **29**

Page intentionally left blank

1 List of Abbreviations

2PI	**T**wo **P**hoton **I**onization
UV	**U**tra **V**iolet
amu	**a**tomic **m**ass **u**nit, $1\,\text{amu} = 1.67 \times 10^{-27}\,\text{kg}$
CCD	**C**harge **C**oupled **D**evice
CMOS	**C**omplementary **M**etal**O**xide**S**emiconductor
CSL	**c**ontinuous **s**pontaneous **l**ocalization
Da	**Da**lton, $1\,\text{Da} \equiv 1\,\text{amu}$
DECIDE	**dec**oherence **i**n a **d**ouble-slit **e**xperiment
DNA	**d**esoxyribo**n**ucleic **a**cid
DPSS	**d**iode-**p**umped **s**olid-**s**tate (laser)
ESI	**e**lectro-**s**pray **i**onization
F2	molecular fluorine (laser)
GRW	**G**hirardi, **R**imini, **W**eber
h	Planck's constant, $h = 6.6 \times 10^{-34}\,\text{Js}$
KDTLI	**K**apitza-**D**irac-**T**albot-**L**au **i**nterferometer
λ_{dB}	deBroglie wavelength
LD	**l**aser **d**esorption
LD-PI	**l**aser **d**esorption followed by **p**hoto **i**onization
LIAD	**l**aser-**i**nduced **a**coustic **d**esorption
LIF	**l**aser **i**nduced **f**luorescence
LITHMOS	**l**aser **i**nduced **th**er**mo**mechanical **s**tress desorption
MALD(I)	**m**atrix-**a**ssisted **l**aser **d**esorption (**i**onization)
MAQRO	**ma**croscopic **q**uantum **r**es**o**nators
NA	**n**ot **a**pplicable
NC	**n**on **c**ritical
Nd:YAG	**n**eo**d**ymium **y**ttrium **a**luminum **g**arnet (laser)
NSE	**N**ewton-**S**chrödinger **e**quation
OTIMA	**o**ptical **t**ime-domain **i**onizing **ma**tter-wave interferometry
QNP	**q**uantum-**n**ano**p**hysics
SAW	**s**urface **a**coustic **w**ave
sCMOS	**S**cientific **C**omplementary **M**etal**O**xide**S**emiconductor
SEM	**s**canning **e**lectron **m**icroscope
SPI	**S**ingle **P**hoton **I**onization
TBD	**t**o **b**e **d**etermined
T_L	**T**albot **l**ength
TLI	**T**albot-**L**au **i**nterferometer
TN	**t**echnical **n**ote

TOF-MS	**T**ime **o**f **F**light **M**ass **S**pectrometer
T_T	**T**albot **t**ime
u	atomic mass **u**nit, $1\,\mathrm{u} \equiv 1\,\mathrm{amu}$
UV	**u**ltra **v**iolet
VCQ	**V**ienna **c**enter for **q**uantum science and technology
vdW	**v**an **d**er **W**aals
VUV	**V**acuum **U**tra **V**iolet, $\lambda < 200\,\mathrm{nm}$

2 Introduction and Motivation

The present study is an experimental investigation of several sources of macromolecules, clusters and nanoparticles, exploring different options for space-based matter-wave experiments, in the future. Interferometry in microgravity and with long coherence times shall enable new tests on the foundations of quantum physics. This includes in particular tests on the linearity of quantum physics with very massive objects - eventually including the interface to gravitational phenomena and mechanisms that transform quantum superpositions into classical observations. A mission in space is expected to enable experiments with particle masses and with a sensitivity to external perturbations far beyond what can be achieved in ground-based experiments.

Matter-wave physics started with theoretical considerations by Louis de Broglie in 1923 [21]. Experimentalists soon demonstrated wave-like behaviour for electrons [20, 64], atoms and molecules [23], as well as neutrons [67]. The quantum-delocalized nature of electrons and neutrons is nowadays routinely exploited in surface-science [65], in the investigation of crystal structures [54], and in the analysis of molecular structures [70].

Recent theoretical proposals have suggest to confirm or falsify a variety of models that modify established quantum theory. Progress in experimental quantum optics in particular in the coherent manipulation of atoms [19], clusters and molecules [35, 39] but also in the preparation of cold nanoparticles [4, 26, 44, 45] is spurring hope that interferometry with particles in the mass range between $10^5 - 10^{10}$ Da may actually become possible. A number of proposals [40–43, 47, 49, 50, 58–61] show how state-of-the-art techniques could be used for testing the foundations of quantum physics using matter-wave interference of massive particles.

The added practical interest in such experiments lies, for example, in technologies that exploit non-classical states of matter in sensors for external forces or internal particle properties [2, 36].

An important motivation for performing matter-wave interferometry with massive objects is to test non-standard modifications of quantum theory[3]. For example, there exist several "macrorealistic" models that predict a transition from quantum to classical behaviour for increasingly massive objects[9, 10, 49]. In particular, macrorealistic models predict decoherence mechanisms that depend quadratically on the mass of the quantum system and to some extent on the distance between the superposed position states. For low-mass particles and small extensions of the quantum wave packet macrorealistic models are indistinguishable from standard quantum theory. If the same experiments can be performed with significantly heavier particles and separations beyond 100 nm, then macrorealistic models predict a transition to classicality, i.e., a decrease in the interference fringe visibility.

Additional modifications of quantum theory have been proposed based on a combination of established quantum mechanics with classical gravity. The solutions of the resulting Einstein-Dirac and Newton-Schrödinger equation [27] also indicate a non-standard evolution of the quantum wave function for objects in excess of 10^{10} amu and for coherence times beyond hours. If at all such conditions can only be realized in dedicated satellite experiments under the best possible

isolation conditions.

Apart from that, nanoparticle interferometry may in the long run also contribute to fundamental experiments that have originally been proposed for atom interferometers in space. This includes tests of the equivalence principle [1, 33, 66] or even the detection of gravitational waves [22, 32].

In contrast to atoms, macromolecules and nanoparticles offer a much richer internal structure. This is at the same time an asset and a drawback. On the positive side, this diversity allows us to reconfigure experimental parameters much more easily in a universal optical matter-wave interferometer[29] than it would be possible in existing atom interferometers. All precision devices use near-resonant atomic transitions and therefore require laser systems optimized for each kind of atom.

In contrast to that, diffraction by non-resonant optical ionization gratings [48, 55] or more general photo-depletion gratings has led to the realization of a new interferometer technique, the OTIMA (optical time-domain ionizing matter-wave) interferometer[30], which is more universally applicable. It works for macromolecules, clusters and nanoparticles. It can be adapted for atoms, too.

At present, nanoparticle interferometry cannot yet compete with atom interferometry when it comes to high-precision measurements. The main reason for that is that nanoparticle sources are orders of magnitude weaker and hotter than present-day atomic beams: their phase-space density is by orders of magnitude smaller than of the well-developed atomic sources. This is similar to the situation of 30 years ago, when electron diffraction was already commercialized and atoms had not yet been cooled. In the mean time, cold atom physics and atom interferometry have been pursued by hundreds of groups around the globe for almost three decades. Compared to that, matter-wave interference with more massive objects is only starting to gain momentum. As of today, macromolecule and cluster interferometry is currently only operative at the Vienna Quantum Nanophysics group (QNP).

Several new groups have started working in this field. Significant progress has for instance been made in cooling the center-of-mass motion of nanoparticles in the size range from $\sim 100\,\mathrm{nm}$ radius [4, 26, 44] up to a few μm radius [45]. This promises two new approaches for matter-wave interferometry with ultra-massive particles. On the one hand, OTIMA-type experiments[31, 35, 50] require cold but not ultra-cold particles. In exchange, the interferometer schemes are delicate. On the other hand, advances in the cooling of nanospheres may open an avenue to ultra-cold objects which provide widely expanding wave functions, intrinsically. [4, 12, 40–43].

3 The proposed experiments

The particle sources explored in the course of this study have been designed with respect to two different types of matter-wave experiments. On the one hand, we propose to use single, optically trapped nanoparticles to investigate decoherence in a double-slit experiment (DECIDE)[40, 41, 43]. On the other hand, we propose to explore quantum delocalization of nanoparticles in an optical time-domain ionizing matter-wave (OTIMA) interferometer [31, 49, 50].

3.1 DECIDE

DECIDE is the central experiment on the proposed medium-sized space mission MAQRO (MAcroscopic Quantum ResOnators, Cosmic Vision call 2010)[43]. In 2012, we completed an ESA-funded study (Po P5401000400) where we investigated DECIDE in greater detail [40]. The goal of DECIDE is to perform experimental tests of the predictions of quantum theory in comparison with the predictions of most macrorealistic models known today. In particular, the experiment should allow to test the CSL model, the models of Diósi and Penrose, a quantum-gravity model proposed by Ellis and coworkers and potentially also the model of Károlyházy [11, 41, 61].

While the optical levitation and manipulation of nano- and microparticles dates back to the 1970s [6–8], the possibility of using such particles for matter-wave interferometry has only recently emerged[16, 58]. In particular, levitated nanospheres have received a remarkable amount of interest since then. Several authors proposed levitated nanospheres for fundamental tests of quantum physics on the ground [57, 59, 61] and in space [40–43]. A first and important step along this way is to cool the center-of-mass motion of trapped nanospheres. Three recent experiments have achieved significant progress towards that goal [26, 44, 45]. If nanoparticles can be cooled to low temperatures, also freely propagating but cavity cooled nanospheres[4] will serve new test of high-mass quantum superpositions [12, 37, 49].

As illustrated in Figure 3.1, the central element of DECIDE is an optical cavity that is used to optically trap a nanosphere with a radius between 50 nm and 120 nm. The nanosphere is fed into the trapping mode from beneath the optical bench via a feed-through (FT) hole in the optical bench. Then the particle is transported along the trapping beam to the trapping position at $\frac{3}{4}$ of the cavity length from the coupling mirror, which also is the position of the cavity waist. Using side-band cooling [24, 46, 68, 69] and feedback cooling (see, e.g., [14, 24, 34]), the center-of-mass (CM) motion of the nanoparticle is cooled close to the ground state of motion along the cavity axis and also to low occupation numbers in the transverse directions. Experiments over the last few years have shown tremendous progress towards achieving that goal. In particular, cooling close to the ground state of motion has recently been achieved for various mechanical systems [15, 51, 63], and promising progress has been made towards achieving the same goal for optically trapped nanoparticles[26, 44, 45].

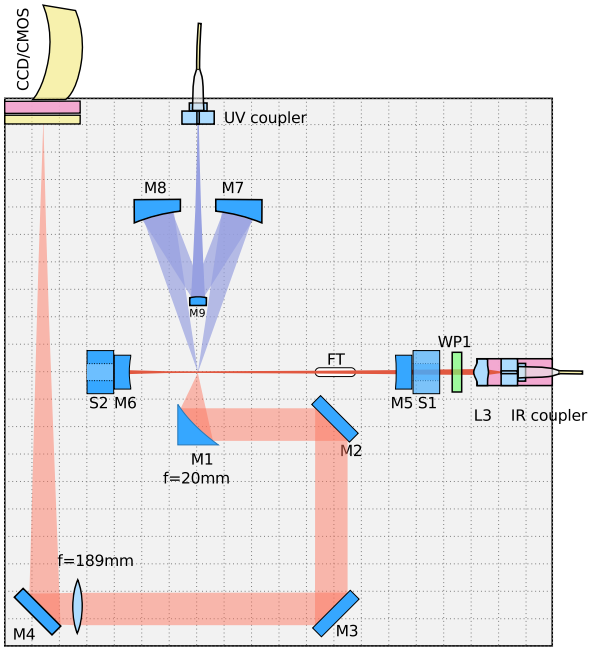

Figure 3.1: Schematic of the optical bench of DECIDE. A polarization maintaining IR fibre supplies two optical modes to the optical cavity. One mode generates the optical trapping field, the second mode can be used for cooling and cavity readout. A very weak ($\sim 10^{-15}$ W) short-wavelength UV beam can be focused at the particle trapping position to prepare a macroscopic superposition. The position of the particle is read out by imaging scattered IR light on a CCD chip [41, 43]. For simplicity, additional modes for feedback cooling have not been included in this schematic layout.

After cooling the particle motion, it is released from the trap and the particle's wavefunction will expand freely for a time t_1 [40, 41, 43, 59, 61]. Then a tightly focused, short-wavelength UV pulse is sent through the center of the wavepacket. If photons are scattered, the particle will be localized. If the particle is far enough from the center of the UV beam, no photons are scattered, and the particle will be in a superposition of being anywhere outside the UV beam waist. The overall quantum state of the nanosphere will then be a mixture of a well localized state and a superposition state.

After this state preparation, the wavepacket will expand freely again for a time $t_2 \gg t_1$. During that time, the two parts of the superposition state (in a 1D picture) will expand, overlap and interfere. To observe the resulting interference pattern, the particle position has to be measured, and the whole process (cooling, expansion, preparation, expansion, position measurement) has to be repeated many times. A histogram of the positions recorded should then show an interference pattern. Due to the localized part of the quantum state (the cases where the UV beam localizes

the nanoparticle) there will be an incoherent background of the interference pattern we want to observe.

The desired result of such an experiment is the visibility of the interference pattern observed, which can be compared with the predictions of quantum theory and with the predictions of alternative theories. By repeating the experiment for various particle sizes and mass densities, it is possible to determine the parameter dependence of the interference visibility and to compare it with the parameter dependence expected from various decoherence effects.

3.2 OTIMA

OTIMA is an interferometer arrangement for manipulating a large class of different materials in a quantum coherent way. It exploits pulsed photo-depletion in a new type of diffraction gratings. The concept is based on the idea [56] that non-resonant photoionization or photo-fragmentation - in particular of clusters or even biomolecules - in an ultraviolet standing light wave can act very similar to a mechanical mask, namely as an absorptive grating [39] that selectively removes particles from certain positions in the beam. Whenever the particles pass a grating antinode they can be ionized, destroyed or transferred into undetected states. The expected diffraction grating will have a period of about 100 nm and is about the smallest structure conceivable with light in this wavelength range.

OTIMA is a particular variant of a Talbot-Lau interferometer(TLI, see Figure 3.2). TLI designs have been known and technically used in classical optics [52] as coherent array illuminators. They were later introduced to atom interferometry [17, 18] and also x-ray optics[53].

Three-grating matter-wave near-field interferometry was first implemented for complex molecules by the QNP group in Vienna [13, 25]. Near-field interferometry makes the instrument compact and stable. Its key advantage, however, is particle throughput. In comparison to far-field schemes including double slit diffraction, it is expected to deliver a thousand times higher throughput, while being even more sensitive to external force fields if so needed.

Near-field interferometry solves a key challenge for all quantum superposition experiments at high or ultra-high mass: It can operate with spatially incoherent sources and beams. The solution of this apparent paradox lies in the fact that the first grating prepares the spatial coherence that is required for wave-like self-imaging of the second grating into a distant plane. The second light grating is responsible for coherent rephasing of the spreading wavelets, and the third one probes the particle density pattern that forms because of quantum interference. This pattern can either be recorded on a screen [38] or be sampled with a third grating.

While matter wave interferometers usually require both spatial and spectral coherence of the incident particle beam, the advantage of OTIMA[31, 35] and KDTLI[25, 35] interferometry consists in the fact that it has only moderate requirements on coherence and thus adapts to a much wider range of particle sources than most other quantum devices demonstrated so far. Transverse coherence is intrinsically correlated with the extension of the particle source: the smaller the source emission area, the wider the transverse coherence further downstream. The nodes of the optical gratings act as many parallel (yet uncorrelated) emitters for nanoparticles and they can reach a width as small as a few nanometers. Moreover, the need for longitudinal coherence is eliminated, to first order, in a non-dispersive interferometer that is operated with

pulsed gratings.

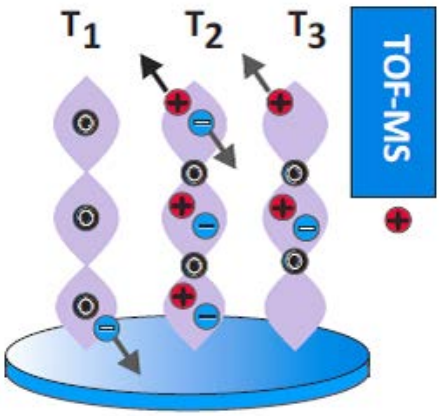

Figure 3.2: Idea of OTIMA interferometry. The three pulsed standing-light-wave gratings in the (V)UV form a near-field interferometer in the time-domain. The first grating (at time T_1) imposes the required spatial coherence of the particle beam. The light pulse at T_2 acts as a complex diffraction grating with an absorptive component and a phase contribution. Quantum interference leads to the formation of a periodic density pattern which is filtered by the standing light wave pulse at T_3. The total transmitted number of particles is recorded and analyzed in a time-of-flight mass spectrometer (TOF-MS).

In addition to removing particles from the beam, the light gratings also add a phase to the matter wave. This phase depends on the light intensity as well as on the particle's polarizability. In experiments that are currently pursued by the QNP group, these gratings are created by the light of three fluorine excimer (F2) lasers that emit at $\lambda = 157.6\,\mathrm{nm}$. They generate diffraction gratings with a period of $d = 79\,\mathrm{nm}$.

Since fluorine lasers are unsuitable for satellite experiments, one needs to consider the use of higher harmonics of pulsed solid-state lasers in the future. One can assume that pulsed lasers in the range of 213 nm will be available for future space experiments. Currently, they already exist in the lab as frequency quintupled Nd:YAG lasers of sufficient power.

OTIMA interferometry requires coherence times on the order of the Talbot time: $T_T = d^2 m/h$. For $\lambda = 213\,\mathrm{nm}$ gratings, this leads to coherence times of the order of 28 ns/amu or about 60 s for objects in the targeted range of 10^9 amu. For free fall on Earth, this corresponds to a height of $\sim$ 18 km. Although it may be possible to devise a levitating-nanoparticle interferometer to compensate for gravitational acceleration, performing such experiments in a micro-gravity environment is clearly appealing.

Over the last years, it has become clear that several high-mass interferometer concepts are well-defined and feasible. While the source developments are making progress, it is still too early to predict whether ground- or space-based experiments will dominate in quantum coherence studies with the most massive objects.

4 Source designs and technical requirements

The present project covered three parallel efforts:

- Exploring laser induced acoustic desorption (LIAD), laser desorption (LD) and laser-induced thermo-mechanical stress (LITHMOS).
- Loading of massive particles into an ion trap. (MALDI Trap)
- Exploration of surface acoustic waves (SAW) for launching ultra-massive particles.

Description	OTIMA	DECIDE
particle radius	$< 50\,\mathrm{nm}$	$\sim 50\,\mathrm{nm} - 120\,\mathrm{nm}$
particle mass density	NC	$2\,\mathrm{g/cm^3} - 10\,\mathrm{g/cm^3}$
particle mass	$10^4\,\mathrm{amu} - 10^9\,\mathrm{amu}$	$10^9\,\mathrm{amu} - 10^{11}\,\mathrm{amu}$
particle species	accessible to, UV-photon-depletion	SiO_2, C, HfO_2 nanospheres
particle shape	NC	spherical
particle temperature	$\leq 1000K$ for $10^4\,\mathrm{amu}$ $\leq 10\,K$ for $10^{10}\,\mathrm{amu}$	$\lesssim 22\,\mathrm{K}$ for $10^{10}\,\mathrm{amu}$
environment temperature	$\leq 20K$ for $10^8\,\mathrm{amu}$	$\lesssim 16\,\mathrm{K}$ for $10^{10}\,\mathrm{amu}$
particle charge in the trap	$1\,\mathrm{e}^-$	NA
particle charge in experiment	$\leq 1\,\mathrm{e}^-$	$0\,\mathrm{e}^-$
particles released per cycle	> 100	$20 < \mathcal{N} < 230$
trapping probability		$\geq 5\%$
max. number of loading cycles	$\sim 10^3$	$\geq 3 \times 10^4$
release velocity	$\leq 100\,\mathrm{m/s}$ for $10^4\,\mathrm{amu}$ scaling with $1/m$	$\leq 20\,\mathrm{mm/s}$
angular spread	NA	$\leq 0.3\,\mathrm{arcmin}$ $\times 3°$
detectable particle fracture	NC	probability $< 10\%$
*un*detectable particle fracture	NA	probability $< 1\%$
source mass	$< 100\,\mathrm{kg}$	$\leq 0.3\,\mathrm{kg}$
source dimensions	likely $50 \times 50 \times 50\,\mathrm{cm^3}$	$5 \times 5 \times 8\,\mathrm{cm^3}$
power consumption	$< 200\,\mathrm{W}$	$< 20\,\mathrm{W}$
thermal requirements	TBD	TBD

Table 4.1: Technical requirements for the loading mechanisms for DECIDE and for OTIMA in space-based matter-wave experiments.

4.1 Technical requirements for the particle sources

Table 4.1 lists the technical requirements that particle sources for the proposed experiments OTIMA and DECIDE ideally have to fulfill. In these first technical demonstrations, not all of these requirements will be fulfilled.

4.2 OTIMA sources

Our goal was to explore the volatilization of nanoparticle using direct LD as well as LIAD – both followed by single-photon ionization (SPI). A similar scheme using laser desorption to load an ion trap was explored as well.

A large range of different molecules was used for the characterization of these methods. They were selected according to the following criteria:

- A well-defined mass facilitates the interpretation for the data and defines the ion trap parameters.
- Thermally stable molecules will survive the desorption process more likely than molecules with labile links. We aimed at good intensities of intact molecules. We have also examined fragile biomolecules in LIAD to explore the softness of the desorption method.
- Photoionizability, preferentially by a single 157 nm photon (SPI) or in two-photon ionization (2PI) at 266 nm is important for particle detection and future quantum manipulation schemes[5]. The VUV wavelength can be provided by a F2 excimer laser. the UV light by via the fourth harmonic of a Nd:YAG laser.

The tests were then performed with Sulforhodamine B (581 Da), Zink-Tetraphenylporphyrin (ZnTPP, 678 Da), tailor-made multi-porphyrines up to 2.5×10^4 Da, oligonucleotides, polystyrene nanoparticles up to 10^7 Da and silicon nanoparticles up to 10^{10} Da.

4.2.1 LD and LIAD

Here, we explore three different molecular sources for the volatilization of molecules of interest which all use pulsed lasers. Through the characterization of these three laser desorption sources we want to test some of the requirements and verify the suitability for space experiments. The molecular sources we investigated throughout this project are MALDI (matrix assisted laser desorption ionization), LD-PI (laser desorption post-ionization) and LIAD. MALDI is mainly used in our ion-trap experiments, and it will be discussed in the trap section since it produces charged molecules. Here, we start by describing the setup for LIAD and LD-PI.

We use a time-of-flight mass spectrometer (Kaesdorf Inc. München) for particle detection as depicted in Figure 4.1. Desorption and post-ionization take place in a vacuum cube with many optical access ports. The sample plate covered with the molecules of interest is placed on an xyz translation stage, which assures that every laser shot hits a fresh sample spot. On the other side of the cube, a load lock chamber is mounted. This helps decreasing the sample exchange time to increase the measurement statistics.

Figure 4.2 depicts the central part of the experiment. The cations are generated inside the repeller volume via a post-ionization laser. In our case, this is a pulsed F2 excimer laser at

157 nm, which is focused into the extraction region via a cylindrical lens. This results in a rectangular beam shape optimized for delivering sufficiently high photon density and ionizing a large fraction of the molecular neutral plume. The photon energy corresponds to approximately 7.89 eV, which is sufficient for single photo-ionization of many organic compounds[62]. Because photo-ionization competes with many relaxation channels in complex particles, we also installed a frequency up-converted pulsed Nd:YAG laser for two-photon ionization at 213 nm and 266 nm.

The molecular desorption takes place several centimeters from the ionization volume. While LD-PI and LIAD correspond to different experimental configurations, the sample preparation is quite similar. In LD-PI, a stainless steel plate is first extensively cleaned and sonicated. Then it is coated with the molecular solution of interest via the dried droplet method and dried out in ambient air. Afterwards, the transfer into the load lock chamber and then into the desorption cube can be made. In LIAD we use thin (8-12.5 μm) and pure ($> 99\%$) metallic foils, usually titanium or tantalum.

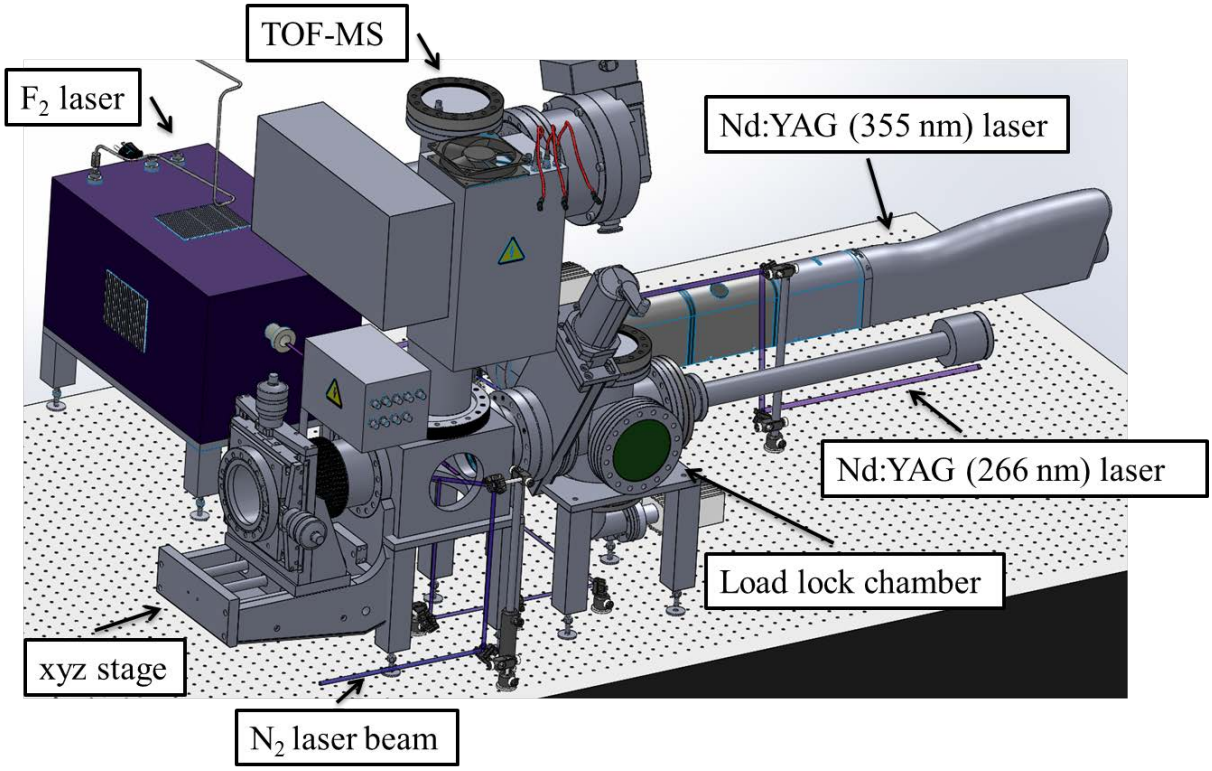

Figure 4.1: Setup for studying LD ionization (LDI) and LIAD. The sample is mounted on an xyz-translation stage to regularly expose fresh sample spots to the N_2 desorption laser. The Nd:YAG laser and the F_2 ($\lambda = 157$ nm) laser provide the pulsed detection. The post-ionized molecules are extracted by a repeller into the time-of-flight mass spectrometer (TOF-MS). A load lock allows fast sample exchange without breaking the vacuum.

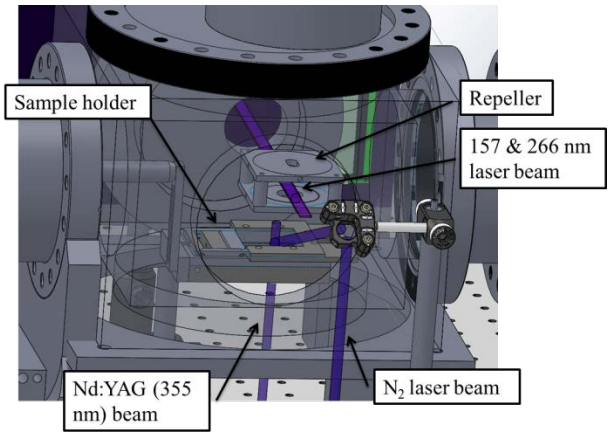

Figure 4.2: Cube where the desorption takes place. A 337 nm laser beam hits the surface of the sample plate for laser desorption with subsequent post-ionization at 157 nm, 266 nm or 213 nm. In case of LIAD, the foil is strained into the sample holder and a 355 nm laser beam desorbs the molecules from sample front surface.

LD-PI is similar to MALDI but it lacks the matrix which would otherwise (de)protonate the analyte molecules in the desorption plume. The absence of acids is better for quantum experiments, as we are interested in neutral species. They are less prone to decoherence by stray electric field fluctuations. Additional non-polar and non-acidic carrier molecules which absorb in the UV may, however, facilitate the launch of nanoparticles as low-velocity propellants.

Compared to MALDI or LD-PI, LIAD is a more recent development [28]. For that, an intense pulsed Nd:YAG laser beam (355 nm) is focused onto the back side of a thin metal foil. A non-thermal mechanism releases the molecules at forward velocities often well below 100 m/s. This technique is believed to be soft since the molecules are not directly exposed to the laser light.

4.2.2 MALDI TRAP

Compared to the previously described LD/LIAD source concept, the MALDI-TRAP design follows a different concept. Here we aim at trapping the particles after their desorption. This shall allow us to select them by mass, as well as to cool them both externally and internally prior to their entrance into the matter-wave interferometer. This provides improved control but it also adds technological challenges. This concept accepts much higher initial energies of the incoming nanoparticles. The trap will dampen the particle motion to the level of their environmental temperature. Reducing the internal temperature lowers also the probability for spontaneous thermal emission and decoherence processes. Fig. 4.3 shows the setup, which was used for testing the suitability of this source. It can be divided into three distinct parts: the source, the ion trap and the detection stage.

MALDI is used to fill the ion trap. A sample plate covered with a suitable mixture of nanoparticles and matrix molecules is placed inside the vacuum chamber, surface face towards the ion trap. Charged particles are desorbed with a pulsed UV laser beam ("1" in Fig. 4.3). For the first

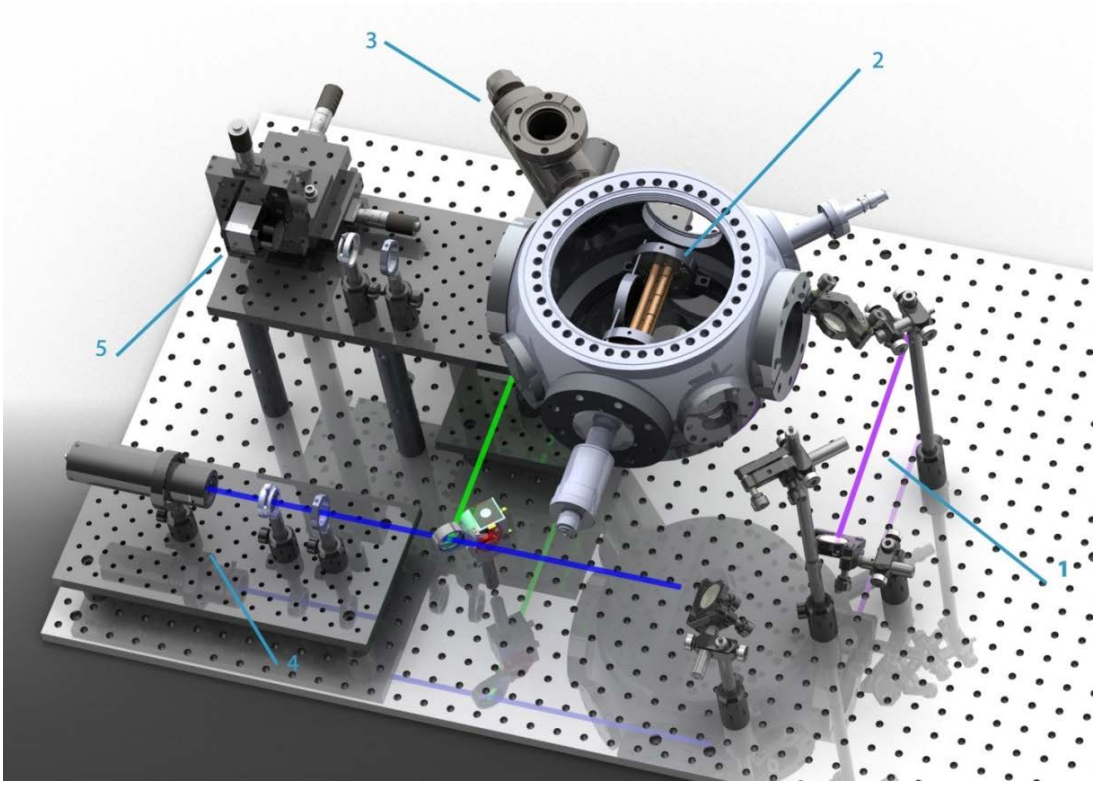

Figure 4.3: Source design of the MALDI-TRAP experiment. The linear quadrupole ion trap (2) is loaded by matrix assisted laser desorption ionization(MALDI) using a pulsed UV laser (1). For efficient thermalization and detection the ion trap can be exposed to a dilute neutral buffer gas (helium) atmosphere. Valve (3) can be pulsed on betwee 100 μs-continuous, if needed. The ions can be imaged onto a sCMOS camera (5) via laser induced fluorescence (LIF). Two excitation lasers (4) at 445 nm and 532 nm are available for that purpose.

characterization of the trap we have used two different kinds of particles: Sulforhodamine B with a mass of 581 Da, for testing the low mass regime and 40 nm diameter polystyrene nanobeads for the ultra-high mass regime. The emitted ions enter a segmented linear quadrupole trap. If the trap is operated at optimal RF settings, the ions can be stably confined for long times. By changing the RF amplitude and frequency, the stability region of the ion trap can be tuned. This allows mass selectivity, as required for the experiment.

Since the ion energy can be quite high in the desorption process, initially, it is necessary to dampen their motion to trap them efficiently. Collisions with light, neutral atoms of a buffer gas at pressures between 10^{-4} and 10^{-3} mbar reduce the kinetic energy of the massive ions. We started the tests using Helium at 300 K, which can be injected via a needle valve for constant residual pressure or via pulsed valve (GV9) to create short ($200 - 2000\,\mu$s) pulses, as shown in Fig. 4.3(3).

A non-destructive ion detector was setup for reading out the status of the ions inside the trapping volume. Laser-induced fluorescence (LIF) has been implemented and tested. Since most molecules and nanoparticles have different excitation and emission lines, we have implemented two lasers, one at 445 nm and one at 532 nm (Fig. 4.3(4)). The blue line is used for polystyrene nanobeads, the green line for Sulforhodamine B.

Since complex molecules have no closed optical transition, they are gradually heated by the Stokes energy which is deposited in every cycle. Therefore, LIF requires a damping mechanism to protect the molecules. To enhance the signal - especially of dilute ion clouds – a buffer gas atmosphere is created inside the trapping volume. The emitted LIF light is collected by a dedicated optical system and imaged onto a sCMOS camera (Fig. 4.3(5)).

4.3 SAW-based particle source

This type of source is based on applying nanoparticles onto the surface of a surface-acoustic-wave (SAW) device. In our case, this was a two-port resonator of the type R2906 supplied to us by the company EPCOS. The idea is that an RF signal (~ 1 GHz) is applied to electrodes on a piezoelectric substrate, which will cause acoustic waves to travel along the surface of the substrate. Nanoparticles attached to the substrate surface follow the transverse movement of the SAWs. This movement leads to accelerations of the nanoparticles proportional to the amplitude of the waves and to the square of the SAW frequency. For a 1 nm amplitude and 1 GHz frequency, this leads to accelerations on the order of 10^9 m/s^2, which should be enough for the particles to desorb from the substrate surface.

The SAW devices we used consisted of SAW substrates contained within ceramic packages with a dimension of $3 \times 3 \times 1$ mm^3. In order to have access to the SAW substrate, we removed the protective lid of the ceramic packages. We mounted the SAW devices on custom-made PCBs as shown in Fig. 4.5.

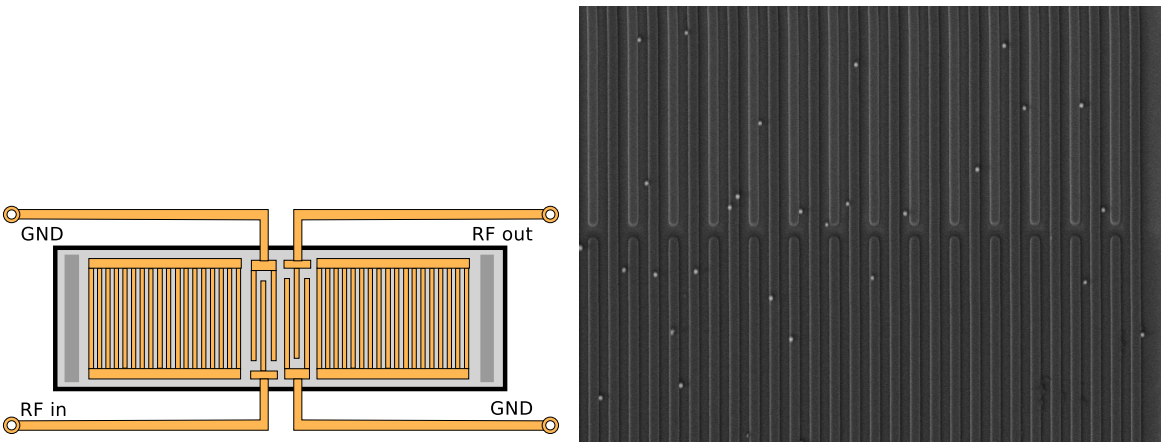

Figure 4.4: **(left)** Schematic of a two-port SAW resonator. Two reflector arrays form a Fabry-Perot cavity. Inside the cavity are two electrode pairs for the radio-frequency (RF) input and output. Dark rectangular shapes to the left and right indicate absorbers to prevent SAw reflections at the substrate edges. **(right)** Scanning electron microscope (SEM) image of a SAW device with 400 nm-diameter fused-silica spheres. The image shows part of one of the reflector arrays of the resonator.

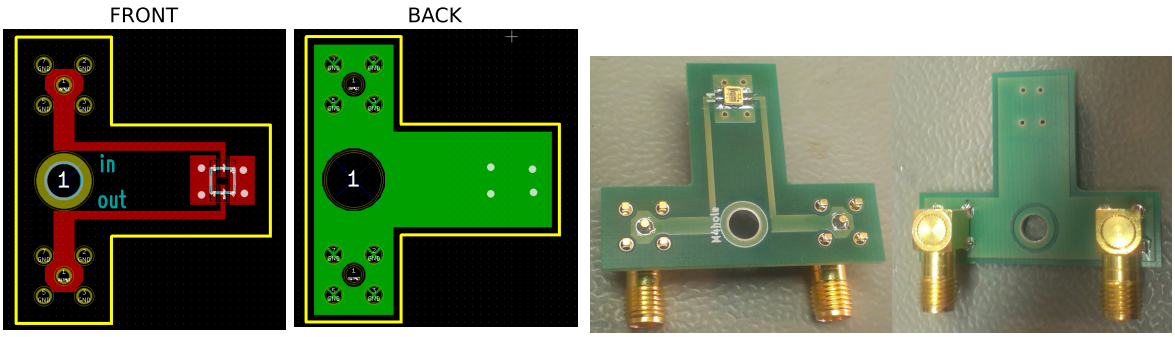

Figure 4.5: **(left)** Front and back view of the printed circuit board (PCB) design for mounting an EPCOS R2906 SAW device. The red and green areas are conductive layers to connect the in and out signals and the ground. The blue rectangle on the front marks the position of the SAW device. Yellow lines indicate the outline of the PCB board. It is 32 mm from left to right and 36 mm from top to bottom. **(right)** Corresponding photos of the a PCB with a SAW device and two SMA connectors in place.

Page intentionally left blank

5 Testing and characterization of the particle sources

5.1 SAW-based particle source

We performed a series of a wide variation of experiments in order to demonstrate the working principle of the SAW-based source, i.e., the desorption of nanoparticles from the SAw substrate. These tests can be divided into three categories: (1) microscope imaging of the SAw substrate, (2) adsorption of desorbed particles on test substrates, (3) direct optical detection of desorbed particles.

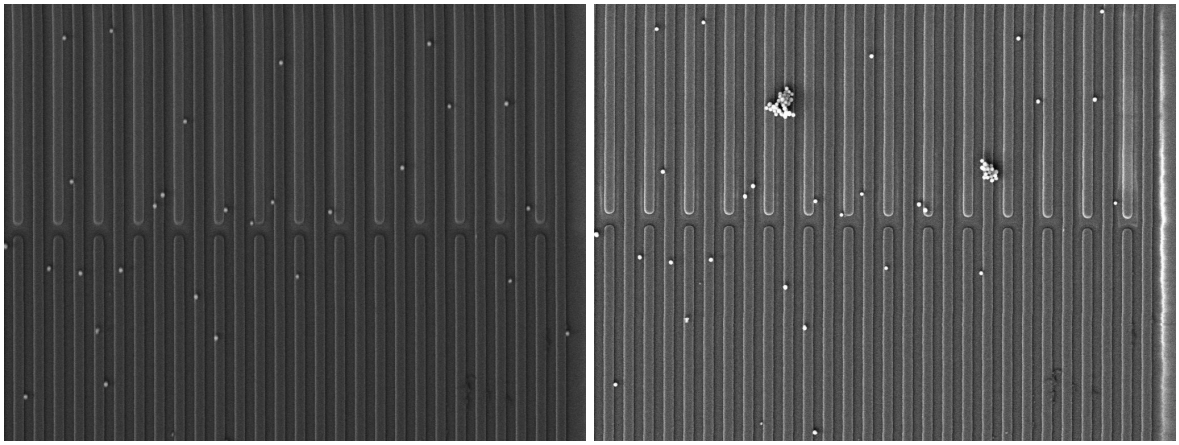

Figure 5.1: SEM images of a SAW substrate covered with 400 nm-diameter fused-silica nanospheres. The long shapes are the reflector electrodes (separation $\sim$ 800 nm, width $\sim$ 900 nm). **(left)** Distribution of particles before applying an RF signal to the SAW device. **(right)** particle distribution after applyint the RF signal. The images show that the SAWs lead to a significant redistribution of the nanoparticles on the substrate.

The most promising results were achieved with method (1) - in particular, with SEM imaging of SAW substrates. For method (2), we placed a microscope slide directly beneath a SAW device such that particles desorbed from the SAW device would be adsorbed on the surface of the microscope slide. Unfortunately, these tests have been non-conclusive so far. However, we want to repeat these tests using fluorescent nanoparticles in the near future. Most our experimental tests were of type (3). Over the course of the present project, we steadily modified

and improved our optical setup to directly detect particles desorbed from SAW devices. The latest setup for optically detecting desorbed (fluorescent) particles is shown in Fig. 5.2.

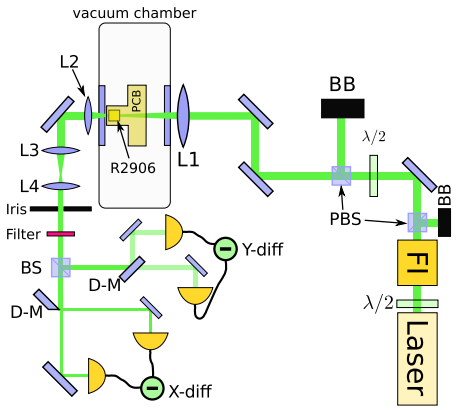

Figure 5.2: Optical setup to detect fluorescent particles desorbed from a SAW device. We use D-shaped mirrors (D-M) to effectively implement a quadrant diode. A fluorescence filter is used to separate the fluorescent light around 620 nm from the excitation wavelength of 532 nm. The same setup without the filter can be used for detecting scattered light. BB: beam block, PBS: polarizing beam splitter, BS: beam splitter, L1-L4: spherical lenses, FI: Faraday isolator

The SAW device was supplied with an RF signal that was generated by a voltage-controlled oscillator (VCO). Before being amplified by a 20 W GHz amplifier, the signal was fed through a variable attenuator. With this scheme, it was possible to operate the SAW device during well-defined, short time intervals. Short operation results in less heating of the SAW substrate and the nanoparticles, and it provides a natural time reference for the time of emission of particles from the source. The recorded data were time traces of the detector signals. In post-processing, we applied a high-pass filter to the data to reject low-frequency noise below 55 Hz. The latest optical setup should, in principle, signal sensitivity that is just high enough to resolve particle desorption events with release velocities up to a few m/s. However, so far, we have not observed any such events. Possible reasons are that (1) the desorbed particles are too fast, (2) the fluorescent particles have bleached too much over time, (3) the optical collection efficiency is lower than assumed, and (4) no particles are desorbed.

5.2 Laser desorption (LD)

For laser desorption/photoionizaiton (LD-PI), a pulsed N_2 laser (337 nm) is focused onto the coated sample plate. It has been tested with a variety of particles (see TN4). We were able to show that this technique is promising for the volatilization of high mass compounds up to 25000 Da with velocities at least down to 20 m/s [62]. This fulfills the requirements for future quantum experiments with high-mass molecules as it leads to de-Broglie wavelengths longer

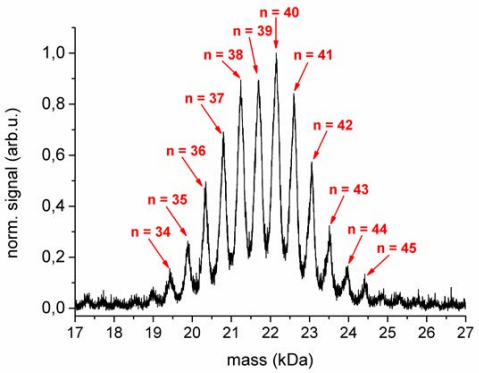

Figure 5.3: LD can lift high-mass, neutral particles into the gas phase – here with masses up to 25000 Da. Properly functionalized (by colleagues at the University of Basel) they can be ionized by a single photon at 157 nm.

than 200 fm, a value already successfully used in earlier OTIMA experiments[31]. It is an open question whether this route can be even continued to substantially higher masses.

5.3 Laser induced acoustic desorption (LIAD)

LIAD was originally meant to be a method for desorbing molecules via acoustic shocks – softer than thermal desorption and therefore better suited for large and potentially thermo-labile particles. However, our experiments have indicated that, in addition to the analyte molecules, substrate nanoparticles may be ejected, too.

This is demonstrated in Fig. 5.4, which shows that a pristine silicon wafer irradiated from its backside, will crack on its front side and even eject 300 nm diameter nanoparticles, occasionally – actually not rarely – also nanospheres. The detailed mechanism still has to be understood. Interestingly, the desorption often occurs at velocities low enough (around 1 mm/s) for us to have been able to observe the first cavity cooling of these particles in high vacuum [4]. This indicates an intriguing avenue for future experiments. Here the plate even does not have to be refilled, as the surface itself transforms into the sample material.

5.4 MALDI TRAP

Loading and stable trapping of the ion trap was another goal of this project. This was fulfilled as demonstrated in 5.5. 40 nm large polystyrene beads could be ejected and charged using MALDI, to be then loaded in the segmented quadrupole ion trap. The high chromophore content of the nanobeads allowed us to record a strong fluorescence signal which shows the joint successful operation of loading, trapping and detection. Future experiments will have to focus on the transfer of the room-temperature sample to a cryogenic ion trap. Internal cooling to 10 K will be crucial for ultra-high-mass quantum interference. This still requires substantial further work.

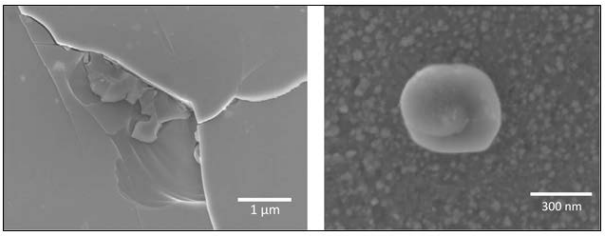

Figure 5.4: Laser induced thermo-mechanical stress LITHMOS releases pristine Silicon nanoparticles of various sizes and shapes, such as for instance this 300 nm nanospheres with a mass of about 10^{10} Da [5]. This mass is the target mass for future quantum experiments in space [35, 49]. The grand challenge remains to cool these objects to internal and external temperatures compatible with quantum delocalization studies.

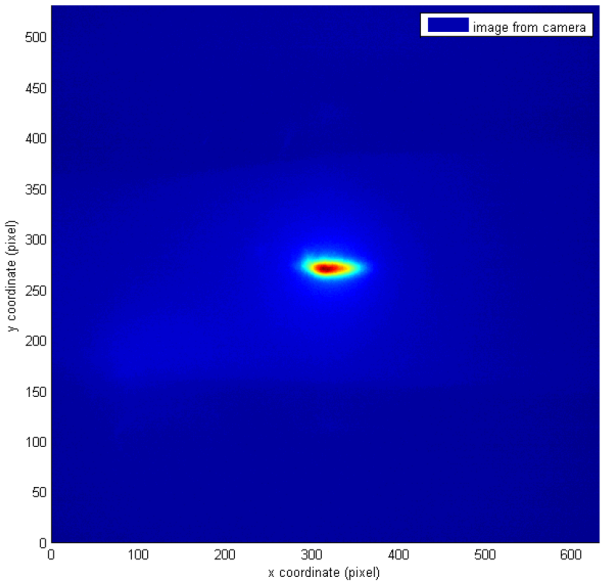

Figure 5.5: MALDI delivers charged polystyrene nanobeads we could trap and observe as bright fluorescent clouds. Radial FWHM: 0.6 mm, length: $\sim$ 4 mm. Assuming a space-charge-limited particle density of $10^6\,\mathrm{cm}^{-3}$ this corresponds to $\sim$ 5000 particles.

6 Trade-off, Conclusions & Discussion

6.1 Trade-off

criterion	LD-PI	LIAD	MALDI-TRAP	SAW
Feasibility	2	2	2	1
Maturity	1	1	1	NC[1]
Applicability	2	2	1	NC[1]
Complexity	1	1	1	2

Table 6.1: **Trade-off between the source mechanisms**. Here, we rate the proposed loading mechanisms and conceptual designs based on the criteria defined within the text. For the ranking, we distribute $1-3$ points, where 3 is the highest ranking. "NC" stands for non-compliant.

Table 6.1 compares the source mechanisms we explored in this project according to the following criteria:

- **Feasibility:**
  How likely is it to successfully achieve the technological requirements in the foreseeable future?
- **Maturity:**
  How mature are the technologies necessary for implementing the various loading mechanisms?
- **Applicability:**
  Are the loading mechanisms applicable for matter-wave experiments that require a space setting?
- **Complexity:**
  How technically challenging is it to implement the proposed loading mechanisms?

[1] These points are marked as non compliant because desorption of nanoparticles would have had to be successfully demonstrated in order to draw proper conclusions about "maturity" and "applicability". This is not a principle limitation, and further experiments and/or technology development may lead to more favorable conclusions about SAW-based sources with respect to these criteria.

6.2 Conclusions & Discussion

In the present project, we have explored a number of possible sources of macromolecules, clusters and nanoparticles for future space-based matter-wave interferometers using massive particles. Our experiments have shown promising results for the proposed particle sources in various regimes of particle types and sizes. Especially, the presented results for the sources for OTIMA show significant progress for particle sources in the mass range of $10^4 - 10^5$ Da. Reliable sources of this type are well on the way, the technology for the corresponding interferometers is ready, and it can be expected that ground-based matter-wave experiments with masses in this range can be realized within the next few years. Results with LIAD even showed impressive progress for masses up to 10^{10} Da. Nevertheless, a significant amount of work will still need to be done until matter-wave interferometry with such high masses will be achievable.

The alternative route of using SAW-based sources for nanoparticles with a mass in the range of $10^9 - 10^{11}$ amu, which we intended to use for DECIDE, also showed some promising results. Yet, so far, we could not conclusively demonstrate that nanoparticles can be made to desorb substrate surfaces by using SAW devices. Still, the current experimental efforts in particle detection as well as in the design of the SAW devices still leaves a lot of room for optimization. If future experiments can demonstrate the successful operation of SAW-based sources, they will, in principle, be well suited for matter-wave interferometry with single particles. On the other hand, the SAW-based source mechanism will not be the best choice for experiments like OTIMA requiring brighter particle sources. This makes it difficult to directly compare the SAW-based source mechanism with the other source mechanisms investigated in this project because they aim at very different experiments.

Based on the promising results of the present project, we are confident that the source concepts presented here will, in the foreseeable future, lead to working sources of high-mass nanoparticles for a variety of new matter-wave experiments on ground and, eventually, also in space.

Bibliography

[1] G. Amelino-Camelia, K. Aplin, M. Arndt, J. Barrow, R. Bingham, C. Borde, P. Bouyer, M. Caldwell, A. Cruise, T. Damour, P. D'Arrigo, H. Dittus, W. Ertmer, B. Foulon, P. Gill, G. Hammond, J. Hough, C. Jentsch, U. Johann, P. Jetzer, H. Klein, A. Lambrecht, B. Lamine, C. Lmmerzahl, N. Lockerbie, F. Loeffler, J. Mendonca, J. Mester, W.-T. Ni, C. Pegrum, A. Peters, E. Rasel, S. Reynaud, D. Shaul, T. Sumner, S. Theil, C. Torrie, P. Touboul, C. Trenkel, S. Vitale, W. Vodel, C. Wang, H. Ward, and A. Woodgate. GAUGE: the GrAnd Unification and Gravity Explorer. *Experimental Astronomy*, 23:549–572, 2009. 10.1007/s10686-008-9086-9. 10

[2] Markus Arndt. De broglie's meter stick: Matter-wave sensing and metrology. *Physics Today*, page in print, 2014. 9

[3] Markus Arndt and Klaus Hornberger. Insight review: Testing the limits of quantum mechanical superpositions. *Nature Physics*, 2014. 9

[4] Peter Asenbaum, Stefan Kuhn, Stefan Nimmrichter, Ugur Sezer, and Markus Arndt. Cavity cooling of free silicon nanoparticles in high vacuum. *Nature Communications*, 4:2743, 2013. 9, 10, 11, 25

[5] Peter Asenbaum, Stefan Kuhn, Stefan Nimmrichter, Ugur Sezer, and Markus Arndt. Cavity cooling of free silicon nanoparticles in high vacuum. *Nature Communications*, 4, October 2013. 26

[6] A. Ashkin. Acceleration and Trapping of Particles by Radiation Pressure. *Phys. Rev. Lett.*, 24(4):156–159, Jan 1970. 11

[7] A. Ashkin. Optical trapping and manipulation of neutral particles using lasers. *Proceedings of the National Academy of Sciences*, 94(10):4853–4860, May 1997.

[8] A. Ashkin and J. M. Dziedzic. Optical Levitation by Radiation Pressure. *Appl. Phys. Lett.*, 19(8):283–285, Oct 1971. 11

[9] A. Bassi and G. Ghirardi. Dynamical reduction models. *Phys. Rep.*, 379:257–426, 2003. 9

[10] Angelo Bassi, Kinjalk Lochan, Seema Satin, Tejinder P. Singh, and Hendrik Ulbricht. Models of wave-function collapse, underlying theories, and experimental tests. *Rev. Mod. Phys.*, 85:471–527, 2013. 9

[11] Angelo Bassi, Kinjalk Lochan, Seema Satin, Tejinder P. Singh, and Hendrik Ulbricht. Models of wave-function collapse, underlying theories, and experimental tests. *Rev. Mod. Phys.*, 85:471–527, Apr 2013. 11

[12] James Bateman, Stefan Nimmrichter, Klaus Hornberger, and Hendrik Ulbricht. Near-field interferometry of a free-falling nanoparticle from a point-like source. *ArXive*, quant-ph/1312.0500v1, 2013. 10, 11

[13] B. Brezger, M. Arndt, and A. Zeilinger. Concepts for near-field interferometers with large molecules. *J. Opt. B*, 5(2):S82–S89, 2003. 13

[14] P. Bushev, D. Rotter, F. Dubin, C. Becher, J. Eschner, R. Blatt, V. Steixner, P. Rabl, and P. Zoller. Feedback Cooling of a Single Trapped Ion. *Phys. Rev. Lett.*, 96:043003, 2 2006. 11

[15] Jasper Chan, T. P. Mayer Alegre, Amir H. Safavi-Naeini, Jeff T. Hill, Alex Krause, Simon Gröblacher, Markus Aspelmeyer, and Oskar Painter. Laser cooling of a nanomechanical oscillator into its quantum ground state. *Nature*, 478(7367):89–92, October 2011. 11

[16] D. E. Chang, C. A. Regal, S. B. Papp, D. J. Wilson, J. Y, O. Painter, H. J. Kimble, and P. Zoller. Cavity opto-mechanics using an optically levitated nanosphere. *Proc. Natl. Acad. Sci. USA*, 107:online publication doi:10.1073/pnas.0912969107, 2009. 11

[17] J. F. Clauser and S. Li. Talbot-von Lau atom interferometry with cold slow potassium. *Phys. Rev. A*, 49:R2213, 1994. 13

[18] J.F. Clauser. *De Broglie-wave interference of small rocks and live viruses, in 'Experimental Metaphysics', Ed. by Cohen, R. S. and Horne, M. and Stachel, J.*, pages 1–11. Kluwer Academic, 1997. 13

[19] Alexander D. Cronin, Jörg Schmiedmayer, and David E. Pritchard. Optics and interferometry with atoms and molecules. *Rev. Mod. Phys.*, 81(3):1051–1129, Jul 2009. 9

[20] C. Davisson and L. H. Germer. The scattering of electrons by a single crystal of nickel. *Nature*, 119:558–560, 1927. 9

[21] Louis de Broglie. Waves and Quanta. *Nature*, 112:540–540, 1923. 9

[22] Savas Dimopoulos, Peter W. Graham, Jason M. Hogan, Mark A. Kasevich, and Surjeet Rajendran. Atomic gravitational wave interferometric sensor. *Phys. Rev. D*, 78:122002, Dec 2008. 10

[23] Immanuel Estermann and Otto Stern. Beugung von Molekularstrahlen. *Z. Phys.*, 61:95–125, 1930. 9

[24] Claudiu Genes, David Vitali, Paolo Tombesi, Sylvain Gigan, and Markus Aspelmeyer. Ground-state cooling of a micromechanical oscillator: comparing cold damping and cavity-assisted cooling schemes. *Phys. Rev. A*, 77:033804, 2008. 11

[25] S. Gerlich, L. Hackermller, K. Hornberger, A. Stibor, H. Ulbricht, M. Gring, F. Goldfarb, T. Savas, M. Mri, M. Mayor, and M. Arndt. A kapitza-dirac-talbot-lau interferometer for highly polarizable molecules. *Nature Physics*, 3(10):711–715, 2007. 13

[26] Jan Gieseler, Bradley Deutsch, Romain Quidant, and Lukas Novotny. Subkelvin Parametric Feedback Cooling of a Laser-Trapped Nanoparticle. *Phys. Rev. Lett.*, 109:103603, Sep 2012. 9, 10, 11

[27] Domenico Giulini and André Großardt. Gravitationally induced inhibitions of dispersion according to the SchrödingerNewton equation. *Classical and Quantum Gravity*, 28(19):195026, 2011. 9

[28] V. V. Golovlev, S. L. Allman, W. R. Garrett, N. I. Taranenko, and C. H. Chen. Laser-induced acoustic desorption. *International Journal of Mass Spectrometry and Ion Processes*, 169-170:69 – 78, 1997. 0168-1176 Matrix-Assisted Laser Desorption Ionization Mass Spectrometry. 18

[29] P. Haslinger et al. An ionizing cluster interferometer in the time domain. in preparation, 2012. 10

[30] Philipp Haslinger, Nadine D"orre, Philipp Geyer, Jonas Rodewald, Stefan Nimmrichter, and Markus Arndt. A universal matter-wave interferometer with optical ionization gratings in the time domain. *Nat. Phys.*, 9:144–148, February 2013. 10

[31] Philipp Haslinger, Nadine Drre, Philipp Geyer, Jonas Rodewald, Stefan Nimmrichter, and Markus Arndt. A universal matter-wave interferometer with optical ionization gratings in the time domain. *Nature Physics*, 9:144–148, 2013. 10, 11, 13, 25

[32] Jason Hogan, David Johnson, Susannah Dickerson, Tim Kovachy, Alex Sugarbaker, Shengwey Chiow, Peter Graham, Mark Kasevich, Babak Saif, Surjeet Rajendran, Philippe Bouyer, Bernard Seery, Lee Feinberg, and Ritva Keski-Kuha. An atomic gravitational wave interferometric sensor in low earth orbit (agis-leo). *General Relativity and Gravitation*, 43:1953–2009, 2011. 10.1007/s10714-011-1182-x. 10

[33] Michael A. Hohensee, Steven Chu, Achim Peters, and Holger Müller. Equivalence Principle and Gravitational Redshift. *Phys. Rev. Lett.*, 106:151102, Apr 2011. 10

[34] Asa Hopkins, Kurt Jacobs, Salman Habib, and Keith Schwab. Feedback cooling of a nanomechanical resonator. *Phys. Rev. B*, 68:235328, 12 2003. 11

[35] K. Hornberger, S. Gerlich, P. Haslinger, S. Nimmrichter, and M. Arndt. Colloquium: Quantum interference of clusters and molecules. *Rev. Mod. Phys.*, 84(1):157–173, 2012. 9, 10, 13, 26

[36] Klaus Hornberger, Stefan Gerlich, Philipp Haslinger, Stefan Nimmrichter, and Markus Arndt. Colloquium: Quantum interference of clusters and molecules. *Rev. Mod. Phys.*, 84:157–173, 2012. 9

[37] T. Juffmann, S. Nimmrichter, M. Arndt, H. Gleiter, and K. Hornberger. New prospects for de broglie interferometry. *Found. Phys.*, 42(1):98–110, 2012. 11

[38] T. Juffmann, S. Truppe, P. Geyer, A.G. Mayor, S. Deachapunya, H. Ulbricht, and M. Arndt. Wave and particle in molecular interference lithography. *Phys. Rev. Lett.*, 103:263601, 2009. 13

[39] Thomas Juffmann, Hendrik Ulbricht, and Markus Arndt. Experimental methods of molecular matter-wave optics. *Rep. Prog. Phys.*, 76:086402, 2013. 9, 13

[40] R. Kaltenbaek, G. Hechenblaikner, et al. Macroscopic quantum experiments in space using massive mechanical resonators. Technical report, Study conducted under contract with the European Space Agency, Po P5401000400, 2011–2012. 9, 10, 11, 12

[41] Rainer Kaltenbaek. Testing quantum physics in space using optically trapped nanospheres. In *Optical Trapping and Optical Micromanipulation X*, volume 8810, page 88100B, 2013. 11, 12

[42] Rainer Kaltenbaek and Markus Aspelmeyer. Optomechanical Schrödinger cats - a case for space. In Reiter, WL and Yngvason, J, editor, *Erwin Schrödinger - 50 Years After*, volume 9 of *ESI Lectures in Mathematics and Physics*, pages 123–134. Europ. Math. Soc., 2013. International Symposium on Erwin Schrodinger - 50 Years After, ESI, Boltzmann Lect Hall, Vienna, ITALY, JAN 13-15, 2011.

[43] Rainer Kaltenbaek, Gerald Hechenblaikner, Nikolai Kiesel, Oriol Romero-Isart, Keith C. Schwab, Ulrich Johann, and Markus Aspelmeyer. Macroscopic quantum resonators (MAQRO). *Experimental Astronomy*, 34:123–164, 2012. 9, 10, 11, 12

[44] Nikolai Kiesel, Florian Blaser, Uros Delic, David Grass, Rainer Kaltenbaek, and Markus Aspelmeyer. Cavity cooling of an optically levitated submicron particle. *Proceedings of the National Academy of Sciences of the United States of America*, 110(35):14180–14185, 2013. 9, 10, 11

[45] Tongcang Li, Simon Kheifets, and Mark G. Raizen. Millikelvin cooling of an optically trapped microsphere in vacuum. *Nature Physics*, 7:527–530, 2011. 9, 10, 11

[46] F. Marquardt, J. P. Chen, A. A. Clerk, and S. M. Girvin. Quantum Theory of Cavity-Assisted Sideband Cooling of Mechanical Motion. *Phys. Rev. Lett.*, 99:093902, 2007. 11

[47] S. Nimmrichter and K. Hornberger. A new measure of macroscopicity. submitted, 2012. 9

[48] Stefan Nimmrichter, Philipp Haslinger, Klaus Hornberger, and Markus Arndt. Concept of an ionizing time-domain matter-wave interferometer. *New Journal of Physics*, 13(7):075002, 2011. 10

[49] Stefan Nimmrichter and Klaus Hornberger. Macroscopicity of mechanical quantum superposition states. *Phys. Rev. Lett.*, 110:160403, 2013. 9, 11, 26

[50] Stefan Nimmrichter, Klaus Hornberger, Philipp Haslinger, and Markus Arndt. Testing spontaneous localization theories with matter-wave interferometry. *Phys. Rev. A*, 83:043621, 2011. 9, 10, 11

[51] A. D. O'Connell, M. Hofheinz, M. Ansmann, R. C. Bialczak, M. Lenander, E. Lucero, M. Neeley, D. Sank, H. Wang, M. Weides, J. Wenner, J. M. Martinis, and A. N. Cleland. Quantum ground state and single-phonon control of a mechanical resonator. *Nature*, 464:697–703, April 2010. 11

[52] K. Patorski. Self-imaging and its applications. In E. Wolf, editor, *Progress in Optics XXVII*, pages 2–108. Elsevier, Amsterdam, 1989. 13

[53] F. Pfeiffer, T. Weitkamp, O. Bunk, and C. David. Phase retrieval and differential phase-contrast imaging with low-brilliance x-ray sources. *Nature Physics*, 2(4):258–261, 2006. 13

[54] David L. Price and Kurt Sköld, editors. *Neutron Scattering, Part B, 23 Experimental Methods in the Physical Sciences*. Academic Press Inc., 1996. 9

[55] E. Reiger, L. Hackermüller, M. Berninger, and M. Arndt. Exploration of gold nanoparticle beams for matter wave interferometry. *Opt. Comm.*, 264:326, 2006. 10

[56] E. Reiger, L. Hackermller, M. Berninger, and M. Arndt. Exploration of gold nanoparticle beams for matter wave interferometry. *Opt. Comm.*, 264:326–332, 2006. 13

[57] O. Romero-Isart, L. Clemente, C. Navau, A. Sanchez, and J. I. Cirac. Quantum Magnetomechanics with Levitating Superconducting Microspheres. eprint arXiv:quant-ph/1112.5609, 2011. 11

[58] O. Romero-Isart, Mathieu L. Juan, Romain Quidant, and J. Ignacio Cirac. Toward quantum superposition of living organisms. *New J. Phys.*, 12:033015, 2010. 9, 11

[59] O. Romero-Isart, A. C. Pflanzer, F. Blaser, R. Kaltenbaek, N. Kiesel, M. Aspelmeyer, and J. I. Cirac. Large Quantum Superpositions and Interference of Massive Nanometer-Sized Objects. *Phys. Rev. Lett.*, 107(2):020405, Jul 2011. 11, 12

[60] O. Romero-Isart, A. C. Pflanzer, M. L. Juan, R. Quidant, N. Kiesel, M. Aspelmeyer, and J. I. Cirac. Optically levitating dielectrics in the quantum regime: Theory and protocols. *Phys. Rev. A*, 83(1):013803, Jan 2011.

[61] Oriol Romero-Isart. Quantum superposition of massive objects and collapse models. *Phys. Rev. A*, 84:052121, Nov 2011. 9, 11, 12

[62] P. Schmid, F. Stohr, M. Arndt, J. Tuxen, and M. Mayor. Single-photon ionization of organic molecules beyond 10 kda. *J Am Soc Mass Spectrom*, 2013. Schmid, Philipp Stohr, Frederik Arndt, Markus Tuxen, Jens Mayor, Marcel ENG 2013/02/28 06:00 J Am Soc Mass Spectrom. 2013 Feb 27. 17, 24

[63] J. D. Teufel, T. Donner, Dale Li, J. W. Harlow, M. S. Allman, K. Cicak, A. J. Sirois, J. D. Whittaker, K. W. Lehnert, and R. W. Simmonds. Sideband cooling of micromechanical motion to the quantum ground state. *Nature*, 475(7356):359–363, July 2011. 11

[64] G. P. Thomson. The Diffraction of Cathode Rays by Thin Films of Platinum. *Nature*, 120:802–802, 1927. 9

[65] M. A. van Hove and S. Y. Tong. *Surface crystallography by LEED*. Springer-Verlag New York, 1979. 9

[66] G. Varoquaux, R.A. Nyman, R. Geiger, P. Cheinet, A. Landragin, and P. Bouyer. How to estimate the differential acceleration in a two-species atom interferometer to test the equivalence principle. *New J. Phys.*, 11:113010, 2009. 10

[67] H. von Halban and P. Preiswerk. Experimental evidence of neutron diffraction. *C.R. Hebd. Séances Acad.*, 203:73, 1936. 9

[68] I. Wilson-Rae, N. Nooshi, J. Dobrindt, T. J. Kippenberg, and W. Zwerger. Cavity-assisted backaction cooling of mechanical resonators. *New J. Phys.*, 10:095007, 2008. 11

[69] I. Wilson-Rae, N. Nooshi, W. Zwerger, and T. J. Kippenberg. Theory of ground state cooling of a mechanical oscillator using dynamical back-action. *Phys. Rev. Lett.*, 99:093901, 2007. 11

[70] Ahmed H. Zewail. 4D Ultrafast electron diffraction, crystallography, and microscopy. *Annual Review of Physical Chemistry*, 57(1):65–103, 2006. 9